Monitoring Carbon Nanotube Growth by Formation of Nanotube Stacks and Investigation of the Diffusion-Controlled Kinetics

Lingbo Zhu,[†] Dennis W. Hess,*[,†] and Ching-Ping Wong*[,‡]

School of Chemical & Biomolecular Engineering, Georgia Institute of Technology, 311 Ferst Drive, Atlanta, Georgia 30332, and School of Materials Science & Engineering, Georgia Institute of Technology, 771 Ferst Drive, Atlanta, Georgia 30332

Received: January 2, 2006; In Final Form: February 2, 2006

A novel method is presented to monitor carbon nanotube (CNT) growth by formation of CNT stacks. By this process, CNT growth kinetics are investigated for densely packed CNT films in the gas-diffusion-controlled regime. CNT stacks are fabricated by water-assisted selective etching and the cyclic introduction of ethylene into the chemical vapor deposition (CVD) reactor. Formation of the CNT stacks allows monitoring of the CNT growth evolution, thereby providing insight into the growth kinetics. A parabolic increase of CNT length versus time is observed, indicating a gas-diffusion-controlled growth mode. The densely packed, well-aligned CNT films act as porous barrier layers to the diffusion of ethylene precursor to the catalyst nanoparticles, since these films form via a base-growth mode under the conditions invoked in our system. By adjustment of CNT growth time and temperature, a quantitative time-evolution analysis is performed to investigate the CNT growth model and extract the gas precursor mass transfer coefficient in the CNT films. The self-diffusion of gases in the densely packed CNT films is found to be Knudsen diffusion with a diffusion coefficient on the order of 10^{-4} cm^2/s.

Introduction

Carbon nanotubes (CNTs) are fascinating one-dimensional molecular structures with interesting and unique properties.[1] In addition to the applications of individual CNTs, a great deal of interest exists to exploit the collective properties of densely aligned CNTs, since such CNT architectures have shown many potential applications in diverse areas such as field emission,[2,3] sensors,[4] and separations.[5,6] Among the various CNT synthesis methods, chemical vapor deposition (CVD) approaches are particularly attractive due to specific CNT growth features such as selective spatial growth, large area deposition capabilities, and aligned CNT growth. As a result, numerous efforts have been made to optimize CVD growth by selecting appropriate catalysts, support layers, carbon precursors, flow rates, and synthesis temperatures and pressures. Also many theories have been proposed to account for observed CNT growth mechanisms.[7−9] Currently, these models focus on the intrinsic CNT growth kinetics, i.e., carbon diffusion into the catalyst nanoparticles and precipitation or formation of graphitic structures when oversaturation occurs. However, the theories have not considered the effect of support materials for the catalysts and thus have not incorporated this parameter into the models. Many reports have shown that the choice of support material is a critical issue for the CVD growth of CNTs.[10−12] Our studies described below demonstrate that selection of appropriate support materials for the catalysts can increase the CNT growth rate by 2 orders of magnitude.

In situ monitoring of CNT growth rates would be helpful to optimize the CNT growth process and explore the mechanisms and kinetics of CNT growth. However, in situ growth characterization is difficult to implement in a CVD reactor, although certain methodologies have been used to gain information. For example, high-resolution in situ transmission electron microscopy (TEM) has been used to observe the formation of CNTs from methane decomposition over supported nickel nanocrystals.[13] However, the TEM environment is different from that of CVD growth, and TEM only observes CNT growth during the initial stages. Other techniques, such as single-slit laser diffractography,[14] optical interference,[15] and time-resolved reflectivity,[9,16] suffer from inefficiencies when measuring thick (long CNT) films and from difficulties in data interpretation and nanotube film surface flatness. We are interested in the growth of extended CNT films (>100 μm) and wish to explore the time dependence of CNT growth. Recently, we reported the formation of carbon nanotubes and stacks of nanotubes by water-assisted selective etching.[17] In this paper, we describe the use of that technique to monitor time-resolved CNT growth. In comparison to other processes to build CNT stacks,[18,19] this process can be adjusted to investigate the diffusion of precursor gases in densely packed CNT films and the CNT growth kinetics in the gas-diffusion-controlled regime. This approach also offers a relatively simple method to circumvent the difficulty of investigation of the intrinsic growth kinetics. Indeed, time-resolved CNT growth behavior could be obtained by varying the growth temperature and the ethylene (carbon precursor) "on" (exposure) time during growth cycles. Furthermore, this process offers a simple way to evaluate the CNT growth behavior from the standpoint of mass transfer of the reaction gases in porous CNT films.

Experimental Details

The detailed experimental procedures used to fabricate CNT stacks were described previously;[17] only a brief description of the process is presented here. Chemical vapor deposition (CVD)

* Authors to whom correspondence should be addressed. Phone: +86-1-404-894-5922 (D.W.H.); +86-1-404-894-8391 (C.-P.W.). Fax: +86-1-404-894-2866 (D.W.H.); +86-1-404-894-9140 (C.-P.W.). E-mail: dennis.hess@chbe.gatech.edu; cp.wong@mse.gatech.edu.

[†] School of Chemical & Biomolecular Engineering.

[‡] School of Materials Science & Engineering.

10.1021/jp060027q CCC: $33.50
Published on Web 02/25/2006

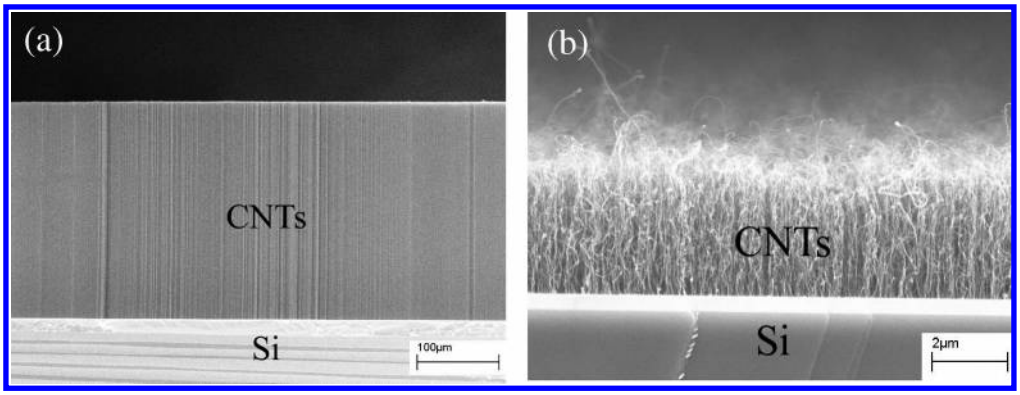

Figure 1. SEM images of as-grown CNTs on a substrate coated (a) with SiO_2 (500 nm)/Al_2O_3 (15 nm) and (b) with only SiO_2 (500 nm).

was performed in a horizontal alumina tube (3.8 cm in diameter; 92 cm in length) housed in a Lindberg Blue furnace. The substrates used in this study were (001) silicon wafers coated with SiO_2 (500 nm) formed by thermal oxidation. The catalyst layers of Al_2O_3 (15 nm)/Fe (1 or 3 nm) were deposited onto the silicon wafer by sequential e-beam evaporation. CVD growth of CNTs was carried out with ethylene (150 sccm) as the carbon source and hydrogen (200 sccm) and argon (350 sccm) as the carrier gases. The water vapor concentration in the CVD chamber was controlled by bubbling a small amount of argon through water held at 22 °C. In all experiments, the water concentration in the furnace tube was maintained at 775 ppm until the CVD process was terminated. The layered CNT films were obtained by the following sequence. Ethylene flowed into the CVD reactor for a preset time, after which the flow was terminated; after 5 min of only water, argon, and hydrogen flow, ethylene was again introduced for a specific time. The fixed 5 min interval between CNT growth steps used water vapor to selectively etch weakly bonded or amorphous carbon atoms existing at the interface between the nanotubes and catalyst particles. Scanning electron microscopy (SEM) studies were performed on a JEOL 1530 equipped with a thermally assisted field emission gun operating at 10 keV.

Results and Discussion

As noted previously, a suitable choice of support material beneath the catalysts is critical in CNT growth. Initially, we employ Al_2O_3 as the catalyst support and compare its effects on CNT growth with a structure wherein only SiO_2 separates the catalyst from the silicon substrate. A 1-nm-thick Fe film is e-beam evaporated onto silicon wafers coated with SiO_2 (500 nm)/Al_2O_3 (15 nm) or with SiO_2 (500 nm). The two diced substrates (5 mm × 5 mm) are positioned in the middle of the CVD tube, and growth of CNTs is carried out at 750 °C for 4 min with ethylene as the carbon source and hydrogen and argon as the carrier gases. Figure 1 shows SEM images of the as-grown CNTs on the two different substrates; significant differences in CNT growth behavior are observed. In Figure 1a, the CNT films attain a height of 267 μm while in Figure 1b the height of the CNT films is only 3.7 μm. These results clearly demonstrate that introduction of the Al_2O_3 support beneath the Fe catalyst increases the CNT growth rate by nearly 2 orders of magnitude under the same growth conditions. Therefore, direct comparison of the intrinsic kinetics of CNT growth with other studies using different support materials is inappropriate.

Through the use of the above recipe for rapid growth of CNTs, it is possible to explore the growth behavior of thick CNT films. For growth of a single-layer CNT film, the CNT growth rate decreases with growth time. However, to establish the time-resolved growth characteristics, in situ monitoring methods or specific growth marks[20] are needed to track the CNT height at a specific time. Recently, we reported a novel process to form carbon nanotube stacks by water-assisted selective etching during growth.[17] By adjusting the ethylene (carbon precursor) cycling times, ethylene exposure times, and growth temperature of this process, we can obtain time-resolved CNT growth behavior. For example, five-layered CNT stacks could be obtained by repeating the growth-etching cycle five times, as shown in Figure 2a. Growth conditions for the CNTs shown in Figure 2a are 80 s of ethylene flow followed by 5 min with the ethylene flow terminated in every cycle at 775 °C with ethylene, argon, and hydrogen flow rates of 150, 350, and 180 sccm, respectively; the Si/SiO_2 substrate had a 3 nm Fe layer deposited onto a 15 nm Al_2O_3 layer. The CNT films in Figure 2a were partially peeled off using tweezers to demonstrate the layered structures of the CNT films, as shown in Figure 2b. CNT layer 1 is the first nanotube layer grown. For growth of CNT layer 2, ethylene must penetrate CNT layer 1, due to the base or root stack growth mechanism.[17] Growth of CNT layer 3 requires the ethylene to penetrate CNT layer 1 and layer 2; analogous processes must occur as additional stacks are added. Diffusion-controlled CNT growth is evident in the decreasing thickness of each subsequent layer. In our reactor/reaction system, since CNT growth occurs by a base-growth mode, ethylene diffuses to the bottom of the CNT films to allow growth on the Fe nanoparticles. Previous investigations have estimated the CNT density in the films under these growth conditions to be approximately 1500 μm^{-2} with an average diameter of 15 nm and a neighboring CNT distance of 30 nm;[12] thus, the CNT films act as densely packed nanoporous layers that present a diffusion barrier to the ethylene precursor. Due to the thick densely packed CNT films (>100 μm) plus the rapid CNT growth rate, the CNT growth rate is controlled by ethylene diffusion through an increasing total CNT film thickness. This effect can be seen in Figure 3c, which shows the individual layer thicknesses. In the first 80 s, the CNT film reaches 155 μm; in the second 80 s, the CNT film grown reaches 140 μm, while the CNT films are 116, 91, and 43 μm in thickness, respectively, during the third, fourth, and fifth 80 s growth cycles. Indeed, for a diffusion-controlled process, the CNT thickness grown for a series of layers is proportional to the square root of time;[20] this relationship is evident in the inset of Figure 2c. When the growth temperature decreases to 725 °C, the CNT growth mode becomes reaction-rate-controlled, as shown in Figure 2d. The growth conditions for the CNTs in Figure 2d are 80 s of ethylene introduction during each growth/etching cycle at 725 °C; all other conditions remained the same as those for films grown at 775 °C. The image shows that the

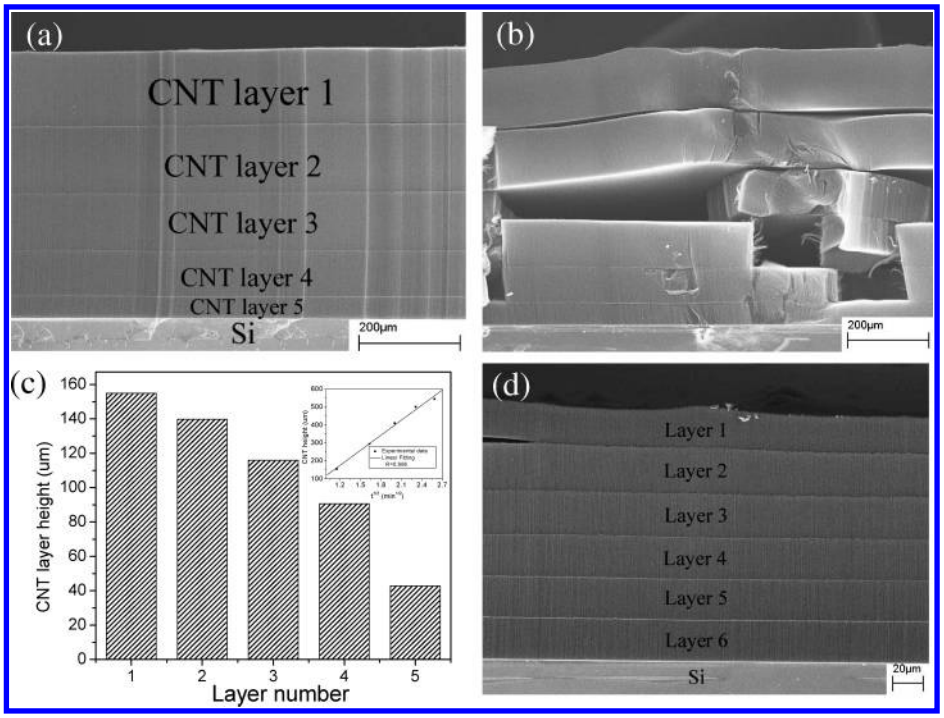

Figure 2. (a) Cross-sectional SEM images of five-layered CNT films. (b) Scratched CNT films from part a to show the layered structures of the CNT films. (c) Individual layer thickness of the CNT films in part a. (d) Cross-sectional SEM image of six-layered CNT films grown in a kinetics-controlled region. The inset in part c shows the linear relationship between CNT film thickness and the square root of growth time, indicating that CNT growth under these conditions is diffusion-controlled.

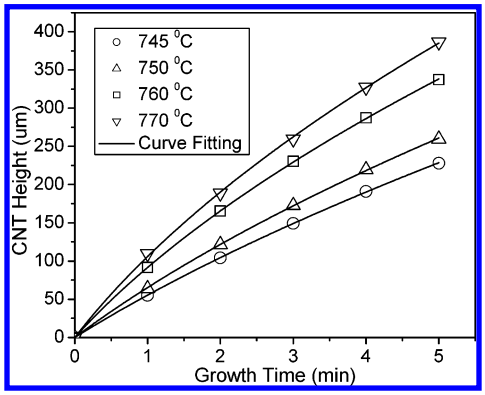

Figure 3. CNT height as a function of growth time at different growth temperatures. The solid line indicates a fit of the experimental data to eq 1.

thickness of the layers is almost the same, except for layer 1, which may be a result of CNT growth latency at the relatively low temperature. The thicknesses of the individual layers are 23.1, 27.7, 27.8, 27.5, 27.5, and 27.5 μm, respectively. If the CNT growth is reaction-rate-limited and we assume a first-order rate process, then the individual layer thicknesses should be linear with time. Our experimental results are in agreement with this assumption. Furthermore, for our reactor/reaction system, CNT growth is observed to be reaction-rate-controlled below 740 °C and diffusion-controlled when the growth temperature exceeds 740 °C.

The diffusion-controlled CNT growth provides a means to obtain additional insight into CNT growth behavior and gas diffusion in the densely packed CNT films. For CNT growth to occur, ethylene must reach the Fe catalyst at the base of the CNT, thereby requiring diffusion through increasingly thicker nanotube films. This process is similar to that observed in the thermal oxidation of silicon, which has been studied extensively. As a result, we model CNT growth in an analogous way; detailed theory and models for silicon oxidation have been described previously.[21,22] The CNT height (h_0) as a function of time (t) can thus be expressed as

$$h_0 = 0.5\sqrt{A^2 + 4Bt} - 0.5A \qquad (1)$$

where $A = 2D/k_s$ and $B = 4DC_0/M$. D is the diffusion coefficient, k_s the first-order rate constant, C_0 the ethylene concentrations at the CNT film surface, and M (mol/μm^3) the number of molecules of ethylene incorporated into a unit volume of the resulting film.

To test the validity of this simple model, we have grown CNT stacks for 1 min of ethylene flow time in each cycle at various temperatures to investigate the time-evolution behavior of CNT growth; all other conditions are those described in the Experimental Section. Figure 3 displays the experimental CNT film height (thickness) as a function of growth time at different temperatures. A fit of eq 1 to the experimental growth time versus thickness data yields excellent agreement ($R^2 = 0.996$) at temperatures of 745, 750, 760, and 770 °C, as shown by the solid lines in Figure 3. We chose the growth temperature to be above 740 °C to ensure CNT growth within the diffusion-controlled regime. By fitting the model equation to the experimental data, the parabolic rate coefficients B and A can be deduced. From B and A, we can also calculate values for the diffusion coefficient D and rate constant k_s. The results of these calculations at the temperatures investigated are summarized in Table 1. The value of C_0 as determined by the gas flow rate is 9.566×10^{-18} mol/μm^3; M is obtained experimentally as 1.091×10^{-15} mol/μm^3 (or 6.571×10^8 molecules/μm^3) from the bulk density (0.0131 g/cm^3) of the as-grown aligned CNT films.

Since the system pressure is uniform in the CVD chamber ($p = 1$ atm), the mass transfer is diffusive in nature and thus may involve ordinary molecular diffusion, Knudsen diffusion, and/or surface diffusion in CNT films. However, surface

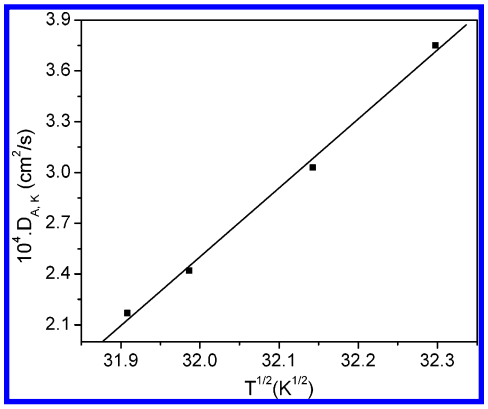

Figure 4. Dependence of the Knudsen diffusion coefficient on temperature.

TABLE 1: Results Summary of Parameters at Various Temperatures

temperature (K)	diffusion coefficient $B \times 10^{-4}$ (μm^2/min)	diffusion coefficient $D \times 10^4$ (cm^2/sec)	A (μm)	k_s (μm/s)
1018.14	4.56	2.17	768	28.3
1023.14	5.09	2.42	714	33.9
1033.14	6.38	3.03	601	50.5
1043.14	7.90	3.75	552	67.9

diffusion will occur only when the diffusion gases are adsorbed in a mobile layer;[23] for these studies, we assume that this transport mode is negligible. If the radius (r) of the channel is small relative to the mean free path (λ), then the rate of mass transport is governed by collisions with the channel walls. This type of transport is usually referred to as Knudsen diffusion. Qualitatively, Knudsen diffusion dominates when the value of r/λ is less than 0.1.[23,24] The mean free path of ethylene is ~181 nm at the same temperature and pressure as our system, as determined from[25]

$$\lambda = \frac{RT}{\sqrt{2}\pi d^2 N_A p} \tag{2}$$

where R is the ideal gas constant (8.314 J/(mol K)), T is temperature (K), d is molecular diameter (4.163×10^{-10} m for ethylene), N_A is Avogadro's number (6.02×10^{23} mol^{-1}), and P is system pressure (101325 Pa). The equivalent diameter of the channels of the CNT films is estimated to be 20 nm by assuming that the diameter and the neighboring distances of the CNTs are 15 and 30 nm, respectively.[12] Therefore, diffusion apparently occurs in the Knudsen regime, since the ratio of channel radius to the mean free path is less than 0.1.

The effective Knudsen diffusivity may be expressed as[25]

$$D_{A,K} = 97.0r\frac{\epsilon}{\tau}\left(\frac{T}{M_A}\right)^{1/2} \tag{3}$$

where r is the channel radius, T is the temperature, ϵ the porosity of the solid, τ the tortuosity factor, and M_A the molecular weight of component A. We do not know exactly values of ϵ and τ, but we assume them to be constant due to the same CNT diameter and area distribution density. According to eq 3, the temperature dependence of the Knudsen diffusion coefficient is proportional to $T^{1/2}$; Figure 4 shows a plot of the diffusion coefficient versus the square root of temperature, indicating a linear relationship between $D_{A,K}$ and $T^{1/2}$. These results suggest that CNT growth under the conditions investigated in this study is controlled by Knudsen diffusion of gases through the densely packed CNT films.

Conclusions

In this paper, CNT stack growth methods are employed to perform a pseudo in situ monitor of CNT growth and gain insight into CNT growth kinetics. By variation of the growth temperature and the ethylene introduction time in growth cycles, a parabolic increase of CNT length versus time is obtained, indicating that gas-diffusion-controlled kinetics establish the intrinsic CNT growth kinetics. Due to the base-growth mode in our reaction/reactor system, the densely packed, well-aligned CNT films act as porous barrier layers to the diffusion of carbon precursors to the catalyst nanoparticles. By variation of the CNT growth temperature, a quantitative time-evolution analysis has been performed based on a simple CNT growth model, thereby allowing determination of the mass transfer coefficient in the CNT films. It was found that a simple kinetics model, similar to the thermal oxidation of silicon, can accurately describe the CNT growth behavior. The diffusion of gases in the spaces between densely packed nanotubes in CNT films is consistent with Knudsen diffusion with a diffusion coefficient on the order of 10^{-4} cm^2/s. These results are important in the modeling of CNT thick film growth and for optimization of the growth parameters.

Acknowledgment. We thank the National Science Foundation for funding support under Contract No. DMI-0422553. We are also grateful to Professor Xinggui Zhou at East China University of Science and Technology for helpful discussions.

References and Notes

(1) Ajayan, P. M. *Chem. Rev.* **1999**, *99*, 1787.
(2) Yoon, S. W.; Kim, S. Y.; Park, J.; Park, C. J.; Lee, C. J. *J. Phys. Chem. B* **2005**, *109*, 20403.
(3) Lee, O. J.; Lee, K. H. *Appl. Phys. Lett.* **2003**, *82*, 3770.
(4) Collins, P. G.; Bradley, K.; Ishigami, M.; Zettl, A. *Science* **2000**, *287*, 1801.
(5) Hinds, B. J.; Chopra, N.; Rantell, T.; Andrews, R.; Gavalas, V.; Bachas, L. G. *Science* **2004**, *3003*, 62.
(6) Srivastava, A.; Srivastava, O. N.; Talapatra, S.; Vajtai, R.; Ajayan, P. M. *Nat. Mater.* **2004**, *3*, 610.
(7) Bartsch, K.; Biedermann, K.; Gemming, T.; Leonhardt, A. *J. Appl. Phys.* **2005**, *97*, 114301.
(8) Louchev, O. A.; Laude, T.; Sato, Y.; Kanda, H. *J. Chem. Phys.* **2003**, *118*, 7622.
(9) Puretzky, A. A.; Geohegan, D. B.; Jesse, S.; Ivanov, I. N.; Eres, G. *Appl. Phys. A* **2005**, *81*, 223.
(10) Hongo, H.; Nihey, F.; Ichihashi, T.; Ochiai, Y.; Yudasaka, M.; Iijima, S. *Chem. Phys. Lett.* **2003**, *380*, 158.
(11) Hongo, H.; Yudasaka, M.; Ichihashi, T.; Nihey, F.; Iijima, S. *Chem. Phys. Lett.* **2002**, *361*, 349.
(12) Zhu, L.; Xu, J.; Xiu, Y.; Sun, Y.; Hess, D. W.; Wong, C. P. *Carbon* **2006**, *44*, 253.
(13) Helveg, S.; López-Cartez, C.; Sehested, J.; Hansen, P. L.; Clausen, B. S.; Rostrup-Nielsen, J. R.; Abild-Pedersen, F.; Nørskov, J. K. *Nature* **2004**, *427*, 426.
(14) Dell'Acqua-Bellavitis, L. M.; Ballard, J. D.; Ajayan, P. M.; Siegel, R. W. *Nano Lett.* **2004**, *4*, 1613.
(15) Kim, D. H.; Jang, H. S.; Kim, C. D.; Cho, D. S.; Yang, H. S.; Kang, H. D.; Min, B. K.; Lee, H. R. *Nano Lett.* **2003**, *3*, 863.
(16) Geohegan, D. B.; Puretzky, A. A.; Ivanov, I. N.; Jesse, S.; Eres, G. *Appl. Phys. Lett.* **2003**, *83*, 1851.
(17) Zhu, L.; Xiu, Y.; Hess, D. W.; Wong, C. P. *Nano Lett.* **2005**, *5*, 2641.
(18) Li, X.; Cao, A.; Jung, Y. J.; Vajtai, R.; Ajayan, P. M. *Nano Lett.* **2005**, *5*, 1997.
(19) Pinault, M.; Pichot, V.; Khodja, H.; Launois, P.; Reynaud, C.; Mayne-L'Hermite, M. *Nano Lett.* **2005**, *5*, 2394.
(20) Liu, K.; Jiang, K.; Feng, C.; Chen, Z.; Fan, S. *Carbon* **2005**, *43*, 2850.
(21) Deal, B. E.; Grove, A. S. *J. Appl. Phys.* **1965**, *36*, 3770.

(22) Jaeger, R. C. *Introduction to Microelectronic Fabrication*; Prentice Hall: Upper Saddle River, NJ, 2002.
(23) Youngquist, G. R. *Ind. Eng. Chem.* **1970**, *62*, 52.
(24) Scott, D. S.; Dullien, F. A. L. *AIChE J.* **1962**, *8*, 113.
(25) Hines, A. L.; Maddox, R. N. *Mass Transfer: Fundamentals and Applications*; Prentice Hall: Englewood Cliffs, NJ, 1985.